5
Robust design optimization with an uncertain model of a nonlinear percussive electromechanical system

The objective of this part of the Thesis is to perform an optimization of a percussive electromechanical system with respect to some chosen design parameters. The optimization consists in maximizing the impact power under the constraint that the electric power consumed by the DC motor is lower than a maximum value. This nonlinear constrained design optimization problem is formulated in the framework of robust design due to the presence of uncertainties in the computational nonlinear dynamics model of the electromechanical system [61, 81, 9].

5.1 Dynamics of the vibro-impact electromechanical system

As described in the introduction, the system is composed by a cart whose movement is driven by the DC motor, and by a hammer that is embarked into the cart. The motor is coupled to the cart through a pin that slides into a slot machined in an acrylic plate that is attached to the cart, as shown in Fig. 5.1. The off-center pin is fixed on the disc at distance Δ of the motor shaft, so that the motor rotational motion is transformed into a cart horizontal movement. To model the coupling between the motor and the mechanical system, the motor shaft is assumed to be rigid. Thus, the available torque vector to the

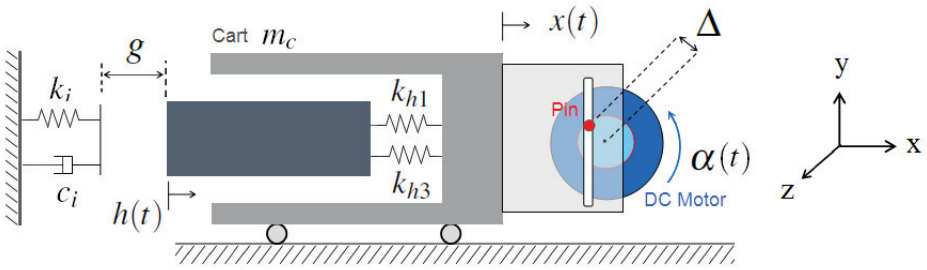

Figure 5.1: Motor-cart-hammer coupled system. The nonlinear component spring is drawn as a linear spring with constant k_{h1} and a nonlinear cubic spring with constant k_{h3}.

coupled mechanical system, $\boldsymbol{\tau}$, can be written as

$$\boldsymbol{\tau}(t) = \boldsymbol{\Delta}(t) \times \mathbf{f}(t)\,, \tag{5.1}$$

where $\boldsymbol{\Delta} = (\Delta\ \cos\alpha(t),\ \Delta\ \sin\alpha(t),\ 0)$ is the vector related to the eccentricity of the pin, and where $\mathbf{f}$ is the coupling force between the DC motor and the cart. Assuming that there is viscous friction between the pin and the slot, the vector $\mathbf{f}$ has two components: the horizontal force that the DC motor exerts in the cart, f_x, and the vertical force, f_y, induced by the viscous friction. The available torque τ and vertical force f_y are written as

$$\tau(t) = f_y(t)\ \Delta\ \cos\alpha(t) - f_x(t)\ \Delta\ \sin\alpha(t)\,, \tag{5.2}$$

$$f_y(t) = c_{pin}\ \Delta\ \dot{\alpha}(t)\ \cos\alpha(t)\,, \tag{5.3}$$

where c_{pin} is the viscous friction. The embarked hammer is modeled as a rigid body of mass m_h and its relative displacement is h with respect to the cart. In the adopted model, the constitutive equation of the spring component between the hammer and the cart is written as $f_s(t) = k_{h1}\ h(t) + k_{h3}\ h(t)^3$. The rate of nonlinearity of the hammer stiffness is defined as $r_h = k_{h3}/k_{h1}$. We introduce the natural frequency, ω_h, of the hammer suspended to the linear spring with constant stiffness k_{h1} such that $\omega_h = \sqrt{k_{h1}/m_h}$. The horizontal cart displacement is represented by x. Due to constraints, the cart is not allowed to move in the vertical direction. The spring-damper element modeling the medium on which the impacts occur, is constituted of a linear spring with stiffness coefficient k_i and a damper with damping coefficient c_i. The equations of the cart-hammer-barrier system were obtained with the Lagrange principle. They are

$$\ddot{x}(t)\ (m_c + m_h) + \ddot{h}(t)\ m_h + c_{ext}\ \dot{x}(t) = -f_{\text{imp}}(t) + f_x(t)\,, \tag{5.4}$$

$$\ddot{x}(t)\ m_h + \ddot{h}(t)\ m_h + c_{int}\ \dot{h} + k_{h1}\ h(t) + k_{h3}\ h^3(t) = -f_{\text{imp}}(t)\,, \tag{5.5}$$

where, c_{ext} is the viscous friction coefficient between the cart and the rail and $c_{int} = 2\varsigma_{int}\sqrt{m_h k_{h1}}$ is the viscous friction coefficient between the cart and the hammer (ς_{int} is the damping ratio). The term f_x is the horizontal coupling force between the DC motor and the cart, and f_{imp} is the impact force between the hammer and the barrier, which is written as

$$f_{\text{imp}}(t) = -\phi(t)\left(\ k_i\ (x(t) + h(t) + g) +\ c_i\ (\dot{x}(t) + \dot{h}(t))\right)\,, \tag{5.6}$$

where

$$\phi(t) = \begin{cases} 1, & \text{if} \quad x(t) + h(t) + g < 0 \quad \text{and} \quad \dot{h}(t) + \dot{x}(t) < 0\,, \\ 0, & \text{in all other cases}\,, \end{cases} \tag{5.7}$$

in which g is defined as the horizontal distance from the hammer (when $\alpha = \pi/2$ rad) to the equilibrium position of the barrier. In the model defined by Eq. (5.7), an impact starts when $x(t)+h(t)$ is negative and equal to $-g$ and, $\dot{h}(t) - \dot{x}(t) < 0$. During an impact, the action of the barrier on the hammer stops as soon as the total velocity $\dot{h}(t) + \dot{x}(t)$ becomes positive (the return of the hammer), i.e, the barrier moves irreversibly in one direction, simulating a penetration. Due to the system geometry, $x(t)$ and $\alpha(t)$ are related by the following constraint

$$x(t) = \Delta \cos(\alpha(t))\,. \tag{5.8}$$

Substituting Eqs. (5.2) to (5.8) into Eqs. (2.1) and (2.2), we obtain the initial value problem for the motor-cart-hammer-barrier coupled system that is written as follows. Given a constant source voltage ν, find (α, c, h) such that, for all $t > 0$,

$$l\dot{c}(t) + rc(t) + k_e\dot{\alpha} = \nu\,, \tag{5.9}$$

$$\begin{aligned} &\ddot{\alpha}(t)\left(j_m + (m_c + m_h)\Delta^2 \sin(\alpha(t))^2\right) - \ddot{h}(t)\left(m_h\Delta \sin(\alpha(t))\right) - k_e c(t) \\ &\quad + \dot{\alpha}(t)\Big(b_m + \dot{\alpha}(t)(m_c + m_h)\Delta^2 \cos(\alpha(t)) \sin(\alpha(t)) \\ &\quad + c_{pin}\Delta^2 \cos(\alpha(t))^2 - c_{ext}\Delta^2 \sin(\alpha(t))^2\Big) \\ &= \phi\left(k_i(\Delta \cos(\alpha(t)) + h + g) + c_i(-d\dot{\alpha}(t) \sin(\alpha(t)) + \dot{h}(t))\right)\Delta \sin(\alpha(t))\,, \end{aligned} \tag{5.10}$$

$$\begin{aligned} &\ddot{h}(t)m_h - \ddot{\alpha}(t)\left(m_h\Delta \sin(\alpha(t))\right) - \dot{\alpha}(t)\left(m_h\Delta\,\dot{\alpha}(t) \cos(\alpha(t))\right) \\ &\quad + \dot{h}(t)c_{int} + k_{h1}h(t) + k_{h3}h^3(t) \\ &= \phi(t)\left(k_i(\Delta \cos(\alpha(t)) + h + g) + c_i(-\Delta\,\dot{\alpha}(t) \sin(\alpha(t)) + \dot{h}(t))\right)\,, \end{aligned} \tag{5.11}$$

where

$$\phi(t) = \begin{cases} 1, & \text{if} \quad \Delta \cos\alpha(t) + h(t) + g < 0 \quad \text{and} \quad \dot{h}(t) - \Delta\,\dot{\alpha}(t) \cos(\alpha(t)) < 0 \\ 0, & \text{in all other cases}\,, \end{cases} \tag{5.12}$$

with the initial conditions,

$$\alpha(0) = 0 \quad , \quad \dot{\alpha}(0) = 0 \quad , \quad c(0) = \frac{\nu}{r} \quad , \quad h(0) = 0 \quad , \quad \dot{h}(0) = 0\,. \tag{5.13}$$

5.2 Dimensionless vibro-impact electromechanical system

In this section, the initial value problem to the vibro-impact electromechanical system is presented in a dimensionless form used for simulations. To get the dimensionless form, we take $\dot{\alpha}(t) = u(t)$ and $\dot{h}(t) = \eta(t)$, and rewrite the initial value problem defined by Eqs. (5.9) to (5.13) as a first order system, as follows

$$\begin{aligned}
\dot{u}(t) = \; & \{-[b_m + m_c\,\Delta^2 u(t)\cos(\alpha(t))\sin(\alpha(t)) + c_{\text{pin}}\,\Delta^2\cos(\alpha(t))^2 \\
& -c_{\text{ext}}\,\Delta^2\sin(\alpha(t))^2]\,u(t)\,m_h + k_e\,c(t)\,m_h - c_{\text{int}}\,\eta(t)\,m_h\,\Delta\sin(\alpha(t)) \\
& -(k_{h1}\,h(t) + k_{h3}\,h^3(t))\,m_h\,\Delta\sin(\alpha(t))\} \\
& /m_h\,(j_m + m_c\,\Delta^2\sin(\alpha(t))^2) \\
\\
\dot{\eta}(t) = \; & \{-[b_m + c_{\text{pin}}\,\Delta^2\cos(\alpha(t))^2 - c_{\text{ext}}\,\Delta^2\sin(\alpha(t))^2]\,u(t)\,m_h\,\Delta\sin(\alpha(t)) \\
& +k_e\,c(t)\,m_h\,\Delta\sin(\alpha(t)) - j_m\,\Delta\,u^2(t)\,\cos(\alpha(t)) \\
& -\phi(t)\,[k_i(\Delta\cos(\alpha(t)) + h(t) + g) + c_i(-\Delta\,u(t)\sin(\alpha(t)) + \eta(t))] \\
& [j_m + m_c\,\Delta\sin(\alpha(t))^2] \\
& -[c_{\text{int}}\,\eta(t) + k_{h1}\,h(t) + k_{h3}\,h^3(t)]\,[j_m + (m_c + m_h)\,\Delta\sin(\alpha(t))^2]\} \\
& /m_h\,(j_m + m_c\,\Delta^2\sin(\alpha(t))^2) \\
\\
c(t) = \; & \frac{1}{l}(\nu - k_e\,u(t) - r\,c(t))
\end{aligned} \tag{5.14}$$

where

$$\phi(t) = \begin{cases} 1, & \text{if} \quad \Delta\cos(\alpha(t)) + h(t) + g < 0 \quad \text{and} \quad \eta(t) - \Delta\,u(t)\sin(\alpha(t)) < 0\,, \\ 0, & \text{in all other cases}\,, \end{cases} \tag{5.15}$$

Writing

$$\begin{aligned}
& t = \frac{l}{r}s, && \alpha\left(\frac{l\,s}{r}\right) = p(s)\,, && u\left(\frac{l\,s}{r}\right) = \frac{r\,q(s)}{l}, \\
& c\left(\frac{l\,s}{r}\right) = \frac{k_e\,w(s)}{l}, && h\left(\frac{l\,s}{r}\right) = \Delta\,a(s)\,, && \eta\left(\frac{l\,s}{r}\right) = \frac{r}{l}\Delta\,y(s)
\end{aligned} \tag{5.16}$$

one gets that s is dimensionless parameter. The functions $p(s)$, $q(s)$, $w(s)$, $a(s)$ and $y(s)$ are dimensionless functions. By substituting the new functions into the Eq. (5.14) one obtains

$$\begin{aligned} q'(s) = \big\{ & -v_3 q(s) - v_1 q^2(s) \cos\left(p(s)\right) \sin\left(p(s)\right) \\ & - v_{12} q(s) \cos\left(p(s)\right)^2 + v_{11} q(s) \sin\left(p(s)\right)^2 + v_2 w(s) \\ & - v_9 y(s) \sin\left(p(s)\right) - \left[v_4 a(s) + v_{18} a^2(s) + v_6 a^3(s)\right] \sin\left(p(s)\right) \big\} \\ & \left\{ \frac{1}{1 + v_1 \sin\left(p(s)\right)^2} \right\} \end{aligned} \tag{5.17}$$

$$\begin{aligned} y'(s) = \big\{ & -v_3 q(s) \sin\left(p(s)\right) - v_{12} q(s) \cos\left(p(s)\right)^2 \sin\left(p(s)\right) + v_{11} q(s) \sin\left(p(s)\right)^3 \\ & + v_2 w(s) \sin\left(p(s)\right) + q^2(s) \cos\left(p(s)\right) - \left[v_{10} + v_9 \sin\left(p(s)\right)^2 (v_8 + 1)\right] y(s) \\ & - \left[v_5 + v_4 \sin\left(p(s)\right)^2 (v_8 + 1)\right] a(s) - \left[v_7 + v_6 \sin\left(p(s)\right)^2 (v_8 + 1)\right] a^3(s) \\ & - \phi(s) \left[(v_{13} + v_{14} v_8 \sin\left(p(s)\right)^2)(\cos\left(p(s)\right) + a(s) + v_{15}) \right. \\ & \left. - (v_{16} + v_{17} v_{18} \sin\left(p(s)\right)^2)(q(s) \sin\left(p(s)\right) - y(s)) \right] \big\} \\ & \left\{ \frac{1}{1 + v_1 \sin\left(p(s)\right)^2} \right\} \end{aligned} \tag{5.18}$$

$$w'(s) = -w(s) - q(s) + v_0 \tag{5.19}$$

$$p'(s) = q(s) \tag{5.20}$$

$$a'(s) = y(s) \tag{5.21}$$

where $'$ denotes the derivative with respect to s and v_i, $i = 0, \ldots, 19$ are dimensionless parameters given by

$$\begin{aligned} & v_0 = \frac{\nu\, l}{k_e\, r}, \quad v_1 = \frac{\Delta^2\, m_c}{j_m}, \quad v_2 = \frac{k_e^2\, l}{j_m\, r^2}, \quad v_3 = \frac{b_m\, l}{j_m\, r}, \quad v_4 = \frac{k_{h1}\, l^2\, \Delta^2}{j_m\, r^2}, \\ & v_5 = \frac{k_{h1}\, l^2}{m_h\, r^2}, \quad v_6 = \frac{k_{h3}\, l^2\, \Delta^4}{j_m\, r^2}, \quad v_7 = \frac{k_{h3}\, l^2\, \Delta^2}{m_h\, r^2}, \quad v_8 = \frac{m_c}{m_h}, \quad v_9 = \frac{c_{int}\, \Delta^2\, l}{j_m\, r}, \\ & v_{10} = \frac{c_{int}\, l}{m_h\, r}, \quad v_{11} = \frac{c_{ext}\, l\, \Delta^2}{j_m\, r}, \quad v_{12} = \frac{c_{pin}\, l\, \Delta^2}{r}, \quad v_{13} = \frac{k_i\, l^2}{m_h\, r^2}, \quad v_{14} = \frac{k_i\, l^2\, \Delta^2}{j_m\, r^2}, \\ & v_{15} = \frac{\mathrm{g}}{\Delta}, \quad v_{16} = \frac{c_i\, l}{m_h\, r}, \quad v_{17} = \frac{c_i\, l\, \Delta^2}{j_m\, r}. \end{aligned} \tag{5.22}$$

5.3 Measure of the system performance

At time t, the electric power introduced by the electrical grid in the motor is

$$\pi_{\text{in}}(t) = \nu\, c(t)\,. \tag{5.23}$$

Let t_b^j and t_e^j be the instants of begin and end of the j-th impact, such that for all t belonging to $[t_b^j\,, t_e^j]$, we have $\dot{x}(t) + \dot{h}(t) < 0$. At time t, the impact power, $\pi_{\text{imp}}^j(t)$, is then written as

$$\pi_{\text{imp}}^j(t) = k_i\,(x(t) + h(t))\,(\dot{x}(t) + \dot{h}(t)), \qquad t_b^j \leq t \leq t_e^j\,. \tag{5.24}$$

The time average of the impact power during the j-th impact, $\underline{\pi}_{\text{imp}}^j$, is written as

$$\underline{\pi}_{\text{imp}}^j = \frac{1}{t_e^j - t_b^j} \int_{t_b^j}^{t_e^j} \pi_{\text{imp}}^j(t)\; dt\,. \tag{5.25}$$

The sum, π_{imp}, of the averages of the impact powers, which is one of the variable of interest in the design optimization problem, is written as

$$\pi_{\text{imp}} = \sum_{j=1}^{N_{\text{imp}}} \underline{\pi}_{\text{imp}}^j\,, \tag{5.26}$$

where N_{imp} is the total number of impacts that occur during time interval $[0, T]$. The time average of the electric power consumed in this time interval is

$$\pi_{\text{elec}} = \frac{1}{T} \int_0^T \pi_{\text{in}}(t)\; dt\,. \tag{5.27}$$

These two variables, π_{imp} and π_{elec}, are chosen to measure the system performance. The biggest π_{imp} is and the smaller π_{elec} is, better will be the system performance.

5.4 Sensitivity analysis and choice of the design parameters

To understand the role played by each system parameter in π_{imp} and π_{elec}, a sensitivity analysis has been done. The objective was to determine what were the system parameters that had the biggest influence in π_{imp} and π_{elec}, in order to define those that will be the design parameters for the robust design optimization problem. The initial value problem defined by Eqs. (5.9) to (5.13) has been rewritten in a dimensionless form for computation and some dimensionless parameters were defined. However, in the sensitivity analysis, these dimensionless parameters were not considered as varying parameters since they do not have an easy physical interpretation. The varying parameters used for the numerical simulations are related with the design of the cart and the embarked hammer. They are:

- m_c/m_h, relation between the hammer mass and the cart mass;
- k_{h1}/m_h, relation between the linear stiffness of the spring component and hammer mass (a sort of natural frequency of the hammer);
- g, horizontal distance from the hammer (when $\alpha = \pi/2$ rad) to the equilibrium position of the barrier;
- Δ, eccentricity of the pin. This parameter determines the length of the cart path.

The other parameters, related with the motor properties and viscous friction coefficients, are fixed and the values of these fixed parameters are given in Table 5.1. The output responses are π_{imp} and π_{elec}. For computation, the

Table 5.1: Values of the system parameters used in simulations.

Parameter	Value	Parameter	Value
m_c	0.50 Kg	ν	2.4 V
r_h	0.30 1/m^2	r	0.307 Ω
c_{pin}	5.00 Ns/m	l	1.88×10^{-4} H
c_{ext}	5.00 Ns/m	j_m	1.21×10^{-4} Kg m^2
ς_{int}	0.05	b_m	1.5452×10^{-4} Nm/(rad/s)
k_i	10^6 N/m	k_e	0.0533 V/(rad/s)
c_i	10^3 Ns/m		

initial value problem defined by Eqs. (5.9) to (5.13) has been rewritten in the dimensionless form given by Eqs. (5.17) to (5.22) . The main objective was to reduce the computation time. Duration is chosen as $T = 10.0$ s. The 4th-order Runge-Kutta method is used for the time-integration scheme for which we have implemented a varying time-step. The time-step is adapted to the state of the dynamical system according to the occurrence or the non occurrence of impacts. When the hammer is not impacting the barrier, the time-step used is 10^{-4} s, but when the hammer is approaching the barrier and when it is impacting it, the time-step is chosen as the value 10^{-5} s. Simulations with different values to the initial conditions, were performed. As it was verified that they do not have a significant influence in π_{imp} and π_{elec}, in all simulations the initial conditions were taken as constant, given by Eq. (5.13). Concerning the sensitivity analysis, $20,000$ numerical simulations have been carried out combining the following values of the parameters: 10 values for m_c/m_h selected in the interval $[0.10\,, 2.00]$, 10 values for k_{h1}/m_h in $[657\,, 4\,410]$ rad^2/s^2, 10 values for g in $[0\,, 0.02]$ m, and 20 values for Δ in $[0.003\,, 0.013]$ m. Due the high numerical cost of these simulations, some strategies were adopted to reduce the computation time:

- the varying time-step integration scheme was used for numerical iterations;
- the initial value problem has been rewritten in a dimensionless form, the computation time of each simulation was reduced from 8 minutes to 5 minutes on average;
- parallelization of the simulations: a cluster in the Laboratoire de Modélisation et Simulation Multi-Echelle of Université Paris-Est with 20 computers was used to make the simulations, as shown in Fig 5.4.

With these strategies, the computational time necessary to perform the $20,000$ numerical simulations were approximately 3.5 days. The largest value of π_{imp},

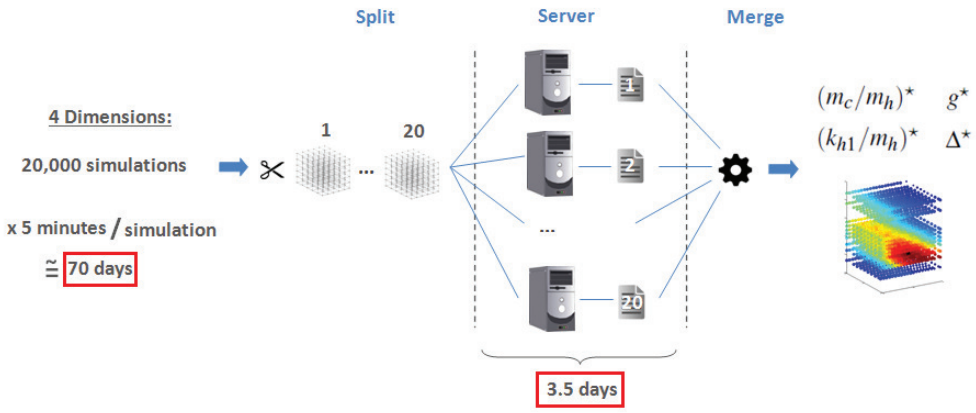

Figure 5.2: Parallelization of the simulations in the sensitivity analysis.

obtained with such numerical simulations, is $5,690$ W, and is reached for the following values of the parameters: $(m_c/m_h)^\star = 0.40$, $(k_{h1}/m_h)^\star = 1,580$ rad^2/s^2, $g^\star = 0.011$ m, and $\Delta^\star = 0.013$ m. With these values, the average of the consumed electric power is $\pi_{\text{elec}} = 3.93$ W. For $\Delta = \Delta^\star$ and $m_c/m_h = (m_c/m_h)^\star$, Fig. 5.3 displays π_{imp} as a function of parameters g and k_{h1}/m_h. In Fig. 5.3(a), g and k_{h1}/m_h vary in all its range of values, and in Fig. 5.3(b), they vary in $[0.06\,,0.02]$ and $[1\,250\,,1\,953]$ respectively. These figures show that, the optimal value of the design parameter correspond to a global maximum. The influence of each parameter in π_{imp} and π_{elec} can be observed through the graphs plotted in Figs. 5.4 to 5.7. Regarding all the graphs of π_{imp} and π_{elec} as a function m_c/m_h, k_{h1}/m_h, g and Δ, it can be seen that small variations on g, k_{h1}/m_h, and Δ induce large variations for π_{imp} and for π_{elec}, but the same phenomenon does not occur with respect to the parameter m_c/m_h. Thus, while π_{imp} and π_{elec} are not very sensitive to m_c/m_h, they are sensitive to k_{h1}/m_h, g and Δ. It is also seen, that two different kinds of sensitivity can be distinguished among these three parameters. For parameters k_{h1}/m_h and g, it can be seen

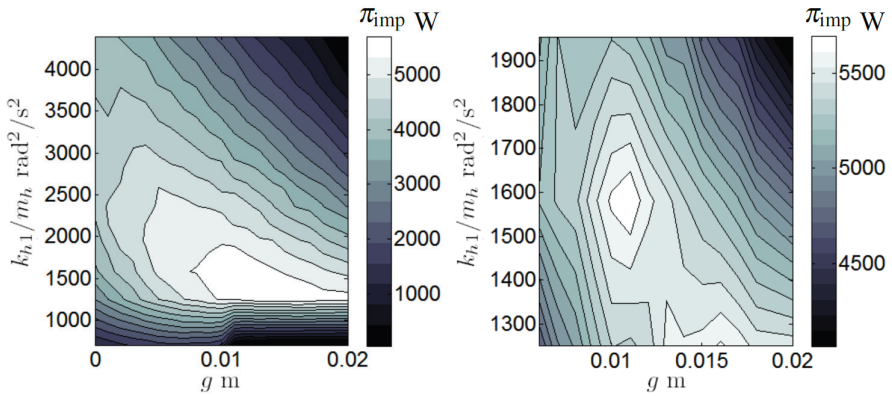

5.3(a): 5.3(b):

Figure 5.3: For the optimal values $(m_c/m_h)^\star$ and $\Delta^\star$: (a) graph of π_{imp} as a function of g and k_{h1}/m_h (varying in all its range of values), (b) graph of π_{imp} as a function of g and k_{h1}/m_h (varying in $[0.06\,,0.02]$ and $[1\,250\,,1\,953]$ respectively).

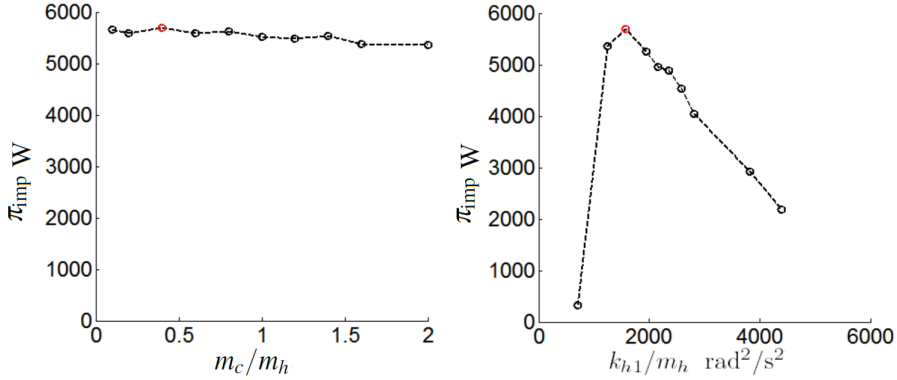

5.4(a): 5.4(b):

Figure 5.4: (a) Graph of π_{imp} as a function of m_c/m_h with $(k_{h1}/m_h)^\star$, $g^\star$, and $\Delta^\star$. (b) Graph of π_{imp} as a function of k_{h1}/m_h with $(m_c/m_h)^\star$, $g^\star$, and $\Delta^\star$.

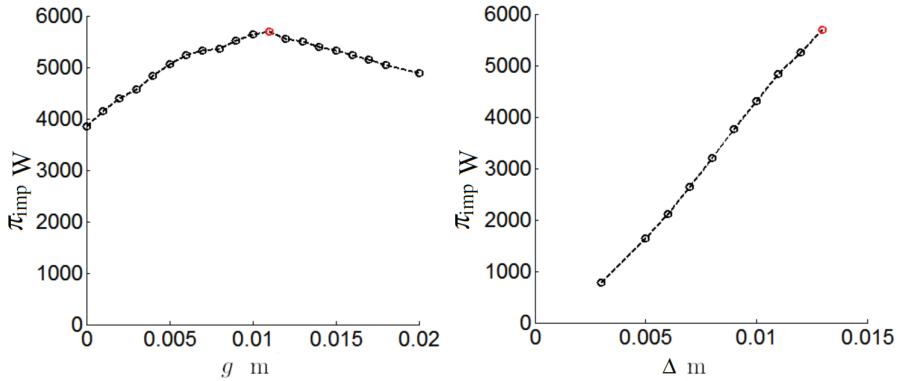

5.5(a): 5.5(b):

Figure 5.5: (a) Graph of π_{imp} as a function of g with $(m_c/m_h)^\star$, $(k_{h1}/m_h)^\star$, and $\Delta^\star$. (b) Graph of π_{imp} as a function of Δ with $(m_c/m_h)^\star$, $(k_{h1}/m_h)^\star$, and $g^\star$.

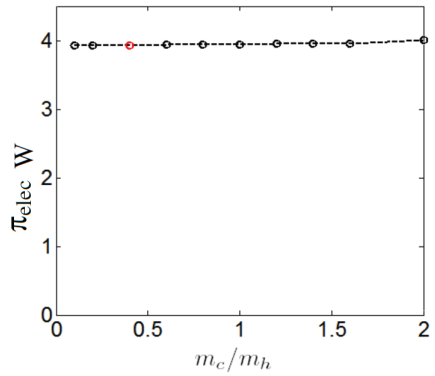

5.6(a):

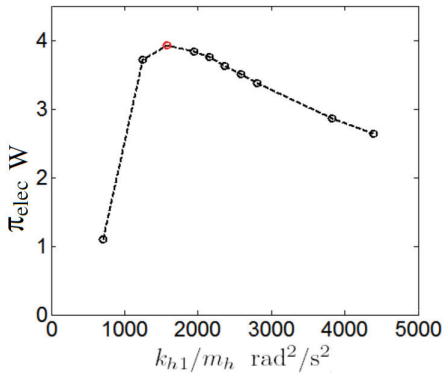

5.6(b):

Figure 5.6: (a) Graph of π_{elec} as a function of m_c/m_h with $(k_{h1}/m_h)^\star$, $g^\star$, and $\Delta^\star$. (b) Graph of π_{elec} as a function of k_{h1}/m_h with $(m_c/m_h)^\star$, $g^\star$, and $\Delta^\star$.

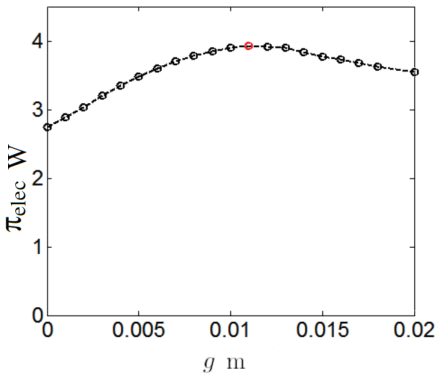

5.7(a):

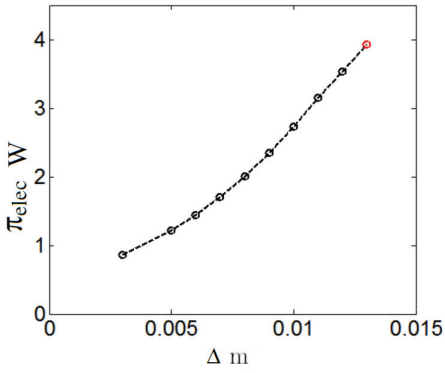

5.7(b):

Figure 5.7: (a) Graph of π_{elec} as a function of g with fix $(m_c/m_h)^\star$, $(k_{h1}/m_h)^\star$, and $\Delta^\star$. (b) Graph of π_{elec} as a function of Δ with fix $(m_c/m_h)^\star$, $(k_{h1}/m_h)^\star$, and $g^\star$.

that π_{imp} and π_{elec} reach their maxima when k_{h1}/m_h and g are equal to $1,580$ rad^2/s^2 and 0.011 m respectively. For parameter Δ varying in its range of values, Figs. 5.5(b) and 5.7(b) show that the highest is Δ, the highest are π_{imp} and π_{elec}. It has been considered as not necessarily to verify the behavior of π_{imp} and π_{elec} for a larger range of Δ because the value $\Delta = 0.013$ m is already sufficiently large when compared with the system dimensions and the motor properties. It should be noted that if parameter Δ is increased, then, the nonlinearities would increase also, but that is not the objective of the analysis. Considering that m_c/m_h does not have a significant influence in π_{imp} and π_{elec}, and considering that the sensitivity of the parameter Δ is easily predictable, these two parameters will not be considered as design parameters in the robust design optimization problem. Only parameters g and k_{h1}/m_h will thus be considered as design parameters.

5.5 Construction of the probability model

As explained in the introduction, this chapter deals with the robust design of the electromechanical system in presence of uncertainties in the computational model. The three parameters that are assumed to be uncertain are k_{h1}, k_i and c_i, which are modeled by the independent random variables K_{h1}, K_i and C_i. The probability distribution of each one is constructed using the Maximum Entropy Principle [34, 88, 89, 91, 85, 94, 95]. This Principle allows the probability distribution of a random variable to be constructed using only the available information, avoiding the use of any additional information that introduces a bias on the estimation of the probability distribution. If a large amount of experimental data are available, then the nonparametric statistics can be used. If there are no available experimental data, or if there are only a few experimental data, then the Maximum Entropy from Information Theory is the most efficient tool for constructing a prior probability model. The Maximum Entropy Principle states: out of all probability distributions consistent with a given set of available information, choose the one that has maximum uncertainty (the Shannon measure of entropy). The available information of the random variables is defined as

1. K_{h1}, K_i and C_i are positive-valued independent random variables,
2. the mean values are known: $E\{K_i\} = \underline{K}_i$, $E\{C_i\} = \underline{C}_i$ and $E\{K_{h1}\} = \underline{K}_{h1}$,
3. in order that the response of the dynamical system be a second-order stochastic process, we impose the following conditions: $\|E\{\log K_i\}\| < \infty$, $\|E\{\log C_i\}\| < \infty$ and $\|E\{\log K_{h1}\}\| < \infty$.

Thus, the Maximum Entropy Principle for each random variable K_i, C_i, and K_{h1}, yields a Gamma distribution (see [90]),

$$p(a) = \mathbb{1}_{[0,+\infty)}(a)\, \frac{1}{\mu} \left(\frac{1}{\delta^2}\right)^{\frac{1}{\delta^2}} \frac{1}{\Gamma(1/\delta^2)} \left(\frac{a}{\mu}\right)^{\frac{1}{\delta^2}-1} \exp\left(\frac{a}{\delta^2 \mu}\right) , \tag{5.28}$$

where $\mathbb{1}_{[0,+\infty)}(a)$ is an indicator function that is equal to 1 for $a \in [0, +\infty)$ and 0 otherwise, and where

- Γ is the Gamma function: $\Gamma(b) = \displaystyle\int_0^\infty t^{b-1} \exp(-t) \mathrm{d}t$;
- $\delta = \frac{\sigma}{\mu}$ is the coefficient variation of the random variable, μ is its mean value representing $\underline{K}_i$, $\underline{C}_i$, or $\underline{K}_{h1}$, and σ is its standard deviation.

5.6 Robust design optimization problem

In order to formulate the robust design problem, the set of all the system parameters is divided into three subsets. The first subset is the family of the fixed parameters that is represented by the vector $\mathbf{p}_{\text{fix}} = \{\, \nu,\ l,\, r,\, j_m,\, k_e,\, b_m,\, c_{pin},\ c_{ext},\, \varsigma_{int},\, r_h,\, m_c,\, m_h,\, \Delta\,\}$. The second one is the family of the design parameters that is represented by the vector $\mathbf{p}_{\text{des}} = \{\underline{K}_{h1}/m_h,\ g\}$. The third one is the family of the uncertain parameters that is represented by the random vector $\mathbf{P}_{\text{unc}} = \{K_i,\ C_i,\ K_{h1}\}$. Since $\mathbf{P}_{\text{unc}}$ is a random vector, the outputs of the electromechanical system are stochastic processes and, consequently, $\pi_{\text{imp}}(\mathbf{p}_{\text{des}}, \mathbf{p}_{\text{unc}})$ and $\pi_{\text{elec}}(\mathbf{p}_{\text{des}}, \mathbf{p}_{\text{unc}})$, become random variables $\Pi_{\text{imp}}(\mathbf{p}_{\text{des}}) = \pi_{\text{imp}}(\mathbf{p}_{\text{des}}, \mathbf{P}_{\text{unc}})$ and $\Pi_{\text{elec}}(\mathbf{p}_{\text{des}}) = \pi_{\text{elec}}(\mathbf{p}_{\text{des}}, \mathbf{P}_{\text{unc}})$. The cost function of the robust design optimization problem is defined by

$$J(\mathbf{p}_{\text{des}}) = E\{\Pi_{\text{imp}}(\mathbf{p}_{\text{des}})\}\,. \tag{5.29}$$

The robust design optimization problem is written as

$$\mathbf{p}_{\text{des}}^{\text{opt}} = \underset{\mathbf{p}_{\text{des}} \in \mathcal{C}_{ad}}{\arg\max}\, J(\mathbf{p}_{\text{des}})\,, \tag{5.30}$$

in which $\mathcal{C}_{ad} = \{\mathbf{p}_{\text{des}} \in \mathcal{P}_{\text{des}};\ E\{\Pi_{\text{elec}}(\mathbf{p}_{\text{des}})\} \leq c_{\text{elec}}\}$, where $\mathcal{P}_{\text{des}}$ is the admissible set of the values of $\mathbf{p}_{\text{des}}$, and where c_{elec} is an upper bound.

5.7 Results of the robust optimization problem

The hyperparameters δ_{K_i} and δ_{C_i}, which control the level of uncertainties for K_i and C_i are fixed to 0.1. The robust design optimization problem is then solved for three levels of uncertainties for K_{h1}, defined by the following values of the hyperparameters $\delta_{K_{h1}} = 0$, $\delta_{K_{h1}} = 0.1$, and $\delta_{K_{h1}} = 0.4$. The optimization problem is also considered whitout uncertainties in the systems parameters, that is, the deterministic case ($\delta_{K_{h1}} = \delta_{K_i} = \delta_{C_i} = 0$). For $\mathbf{p}_{\text{des}} \in \mathcal{C}_{ad}$, the cost function is estimated by the Monte Carlo simulation method using 100 independent realizations of random vector $\mathbf{P}_{\text{unc}}$ following its probability distribution. The optimization problem (defined by Eq. (5.30)) is solved using the trial method for which the admissible set $\mathcal{C}_{ad}$ is meshed as follows: for $\underline{K}_{h1}/m_h$, 13 values are nonuniformly selected in the interval $[703\,,3\,830]$, and for g, 20 nonuniform values in $[0\,,0.038]$. Thus, $26,000$ numerical simulations have been carried out to solve optimization problem for each level of uncertainties. Due the high numerical cost of these simulations, the same strategies used in the sensitivity analysis were adopted to reduce the computation time. They were:

- a varying time-step integration scheme was used for numerical iterations (described in Section 5.4 with duration $T = 10.0$ s),
- the initial value problem has been rewritten in a dimensionless form, the computation time of each simulation was reduced from 8 minutes to 5 minutes on average;
- parallelization of the simulations: a cluster in the Laboratoire de Modélisation et Simulation Multi-Echelle of Université Paris-Est with 20 computers was used to make the simulations.

These strategies allowed us to solve the optimization problem (defined by Eq. (5.30)) with the trial method. With the reduction of computation time, different kind of algorithms, as evolutionary algorithms or random search algorithm were not necessary. The computational time necessary to perform the 26,000 numerical simulations were approximately 4.5 days for each level of uncertainties. The values of the fixed parameters are $m_c = 0.3$ Kg, $m_h =$

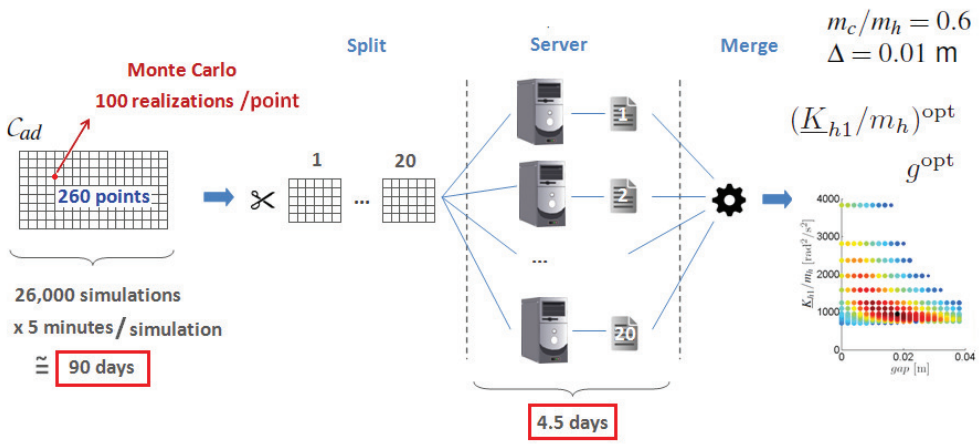

Figure 5.8: Parallelization of the simulations performed to solve the robust optimization problem.

0.5 Kg, $\Delta = 0.01$ m, and the others are given in Table 5.1. Upper bound c_{elec} is fixed to the value 6.00 W. For the deterministic case, the components of the optimal solution $\mathbf{p}_{\text{des}}^{\text{opt}}$ are $(\underline{K}_{h1}/m_h)^{\text{opt}} = 1,580$ rad^2/s^2 and $g^{\text{opt}} = 0.011$ m. For case with uncertainties, for which δ_{K_i} is fixed to 0.1, and δ_{C_i} to 0.1, we obtain, for $\delta_{K_{h1}} = 0$, $(\underline{K}_{h1}/m_h)^{\text{opt}} = 957$ rad^2/s^2 and $g^{\text{opt}} = 0.018$ m, for $\delta_{K_{h1}} = 0.1$, $(\underline{K}_{h1}/m_h)^{\text{opt}} = 1,950$ rad^2/s^2 and $g^{\text{opt}} = 0.008$ m, and for $\delta_{K_{h1}} = 0.4$, $(\underline{K}_{h1}/m_h)^{\text{opt}} = 2,360$ rad^2/s^2 and $g^{\text{opt}} = 0.008$ m. Figures 5.9 and 5.10 display the graphs of the cost function defined by Eq. (5.29) as a function of the design parameter for these four cases. These figures show that, for each case, the optimal value of the design parameter correspond to a global maximum in $\mathcal{C}_{ad}$. The role played by uncertainties on the optimal values of the design

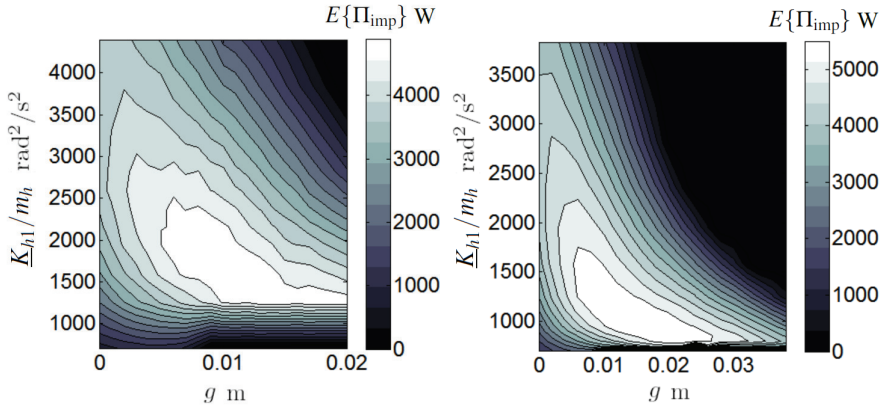

5.9(a): 5.9(b):

Figure 5.9: (a) Cost function as function of the design parameters for the deterministic case. (b) Cost function as function of the design parameters for the case in which $\delta_{K_i} = \delta_{C_i} = 0.1$ and $\delta_{K_{h1}} = 0$.

parameters can be analyzed through Figs. 5.11 and 5.12, which display the graphs $g \mapsto E\{\Pi_{\text{imp}}((\underline{K}_{h1}/m_h)^{\text{opt}}, g)\}$, $\underline{K}_{h1}/m_h \mapsto E\{\Pi_{\text{imp}}(\underline{K}_{h1}/m_h, g^{\text{opt}})\}$, $g \mapsto E\{\Pi_{\text{elec}}((\underline{K}_{h1}/m_h)^{\text{opt}}, g)\}$, and $\underline{K}_{h1}/m_h \mapsto E\{\Pi_{\text{elec}}(\underline{K}_{h1}/m_h, g^{\text{opt}})\}$. These figures show that the optimal design point strongly depends on the level of uncertainties. In particular, it can be deduced that the mean value of the electric power increases with the increase of the gap. The robustness of the optimal design point, $\mathbf{p}_{\text{des}}^{\text{opt}}$, can be analyzed in studying the evolution of the coefficient variation, $\delta_{\Pi_{\text{imp}}}(\mathbf{p}_{\text{des}}^{\text{opt}})$, of random variable $\Pi_{\text{imp}}(\mathbf{p}_{\text{des}}^{\text{opt}})$ as a function of the uncertainty level. However, in order to better analyze the sensitivity of the responses with respect to the uncertainty level, we have constructed Fig. 5.13 that displays the graphs $g \mapsto \delta_{\Pi_{\text{imp}}}((\underline{K}_{h1}/m_h)^{\text{opt}}, g)$ and $\underline{K}_{h1}/m_h \mapsto \delta_{\Pi_{\text{imp}}}(\underline{K}_{h1}/m_h, g^{\text{opt}})$. For each level of uncertainties, it can be seen that the value $\delta_{\Pi_{\text{imp}}}(\mathbf{p}_{\text{des}}^{\text{opt}})$ occurs in a region for which the two following functions $g \mapsto \delta_{\Pi_{\text{imp}}}((\underline{K}_{h1}/m_h)^{\text{opt}}, g)$ and $\underline{K}_{h1}/m_h \mapsto \delta_{\Pi_{\text{imp}}}(\underline{K}_{h1}/m_h, g^{\text{opt}})$ are minima. This means the optimal design point is robust with respect to uncertainties.

5.8 Summary of the Chapter

In this chapter of the Thesis, the formulation and the solution of a robust design optimization problem have been presented for a nonlinear electromechanical vibro-impact system in presence of uncertainties in the computational model. Since this nonlinear electromechanical system is devoted to the vibro-impact optimization, the time responses exhibit numerous shocks that have to be identified with accuracy, and consequently, a very small time-step is re-

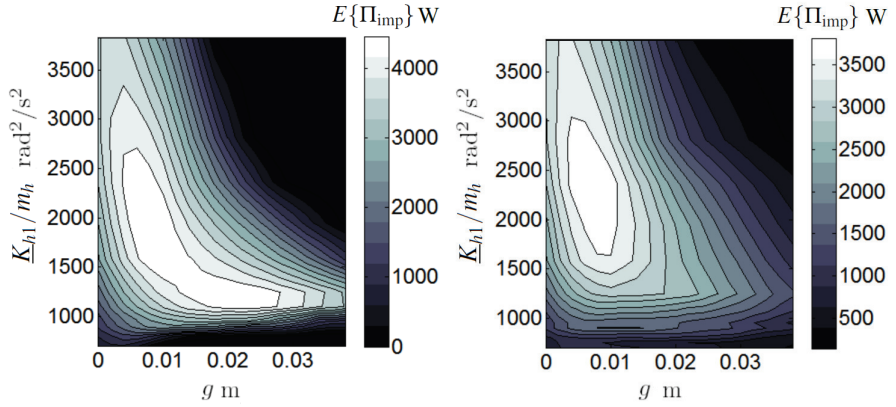

5.10(a): 5.10(b):

Figure 5.10: (a) Cost function as function of the design parameters for the case in which $\delta_{K_i} = \delta_{C_i} = \delta_{K_{h1}} = 0.1$. (b) Cost function as function of the design parameters for the case in which $\delta_{K_i} = \delta_{C_i} = 0.1$ and $\delta_{K_{h1}} = 0.4$.

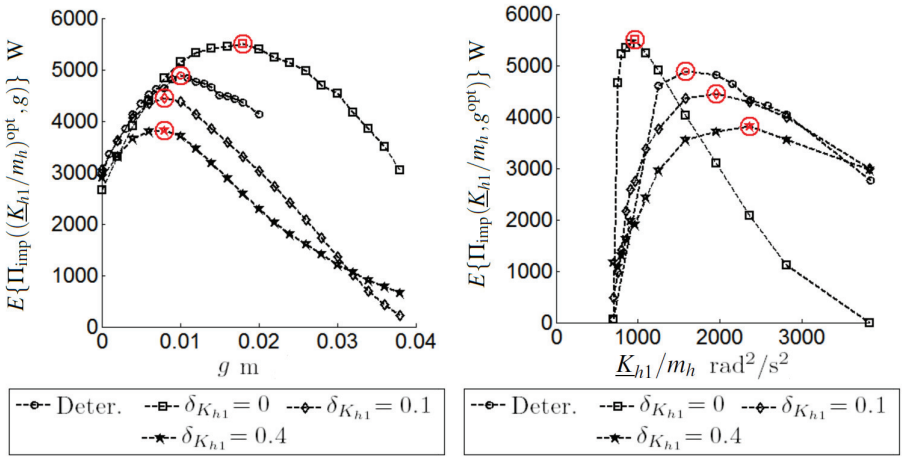

5.11(a): 5.11(b):

Figure 5.11: (a) Cost function as function of g with $(\underline{K}_{h1}/m_h)^{\text{opt}}$. (b) Cost function as function of $\underline{K}_{h1}/m_h$ with g^{opt}. In both graphs, the $E\{\Pi_{\text{imp}}(\mathbf{p}_{\text{des}}^{\text{opt}})\}$ is highlighted for each level of uncertainties with markers.

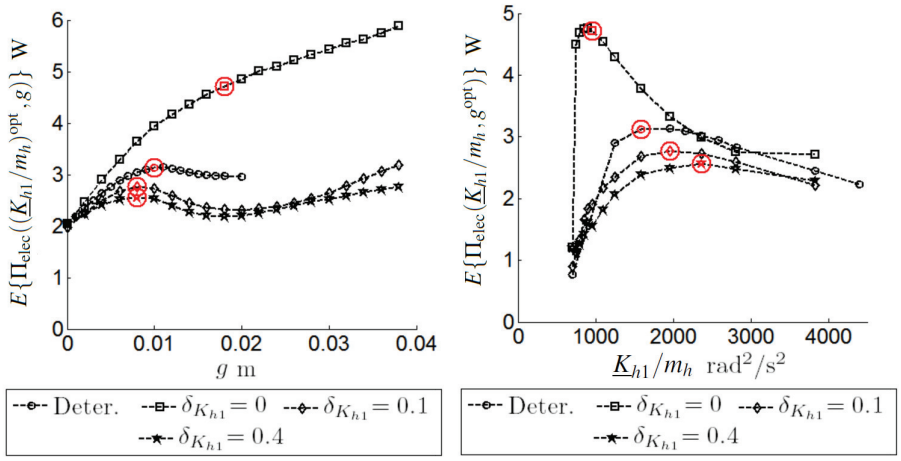

5.12(a): 5.12(b):

Figure 5.12: (a) Mean value of the time average of electric power as function of g with $(\underline{K}_{h1}/m_h)^{\text{opt}}$. (b) Mean value of the time average of electric power as function of $\underline{K}_{h1}/m_h$ with g^{opt}. In both graphs, the $E\{\Pi_{\text{elec}}(\mathbf{p}_{\text{des}}^{\text{opt}})\}$ is highlighted for each level of uncertainties with markers.

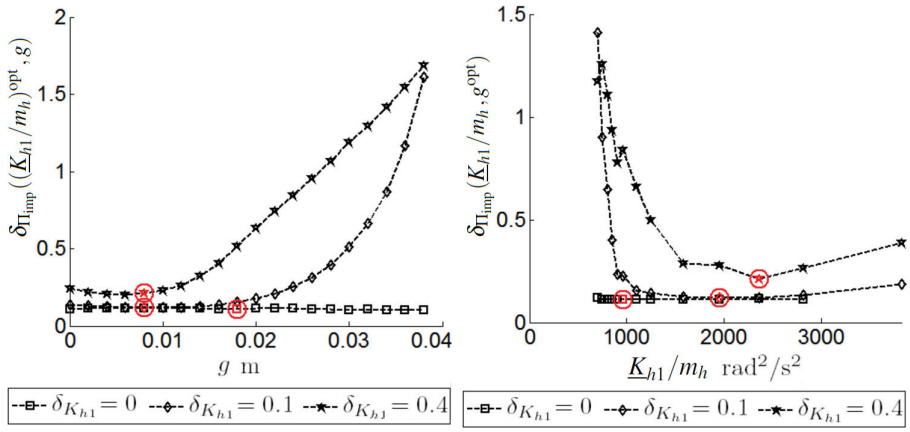

5.13(a): 5.13(b):

Figure 5.13: (a) Coefficient variation of Π_{imp} as function of g with $(\underline{K}_{h1}/m_h)^{\text{opt}}$. (b) Coefficient variation of Π_{imp} as function of $\underline{K}_{h1}/m_h$ with g^{opt}. In both graphs, the $\delta_{\Pi_{\text{imp}}}(\mathbf{p}_{\text{des}}^{\text{opt}})$ is highlighted for each level of uncertainties with markers.

quired. We have thus chosen an explicit time-integration scheme and not an implicit one. Nevertheless, due to the presence of low-frequency contributions in the time responses, a long time duration is required, which will imply a huge number of integration time-step if the time-step was chosen constant. This is the reason why we have implemented an adaptive integration time-step. It was one of the difficulties encountered for the solver implementation. The use a varying time-step integration scheme was not the only strategy adopted to reduce the computation time. The initial value problem has been rewritten in a dimensionless form, which reduced the computation time of each simulation from 8 minutes to 5 minutes on average. Furthermore, a cluster with 20 computers has been used to to parallelize the simulations carried out in the sensitivity analysis and in the optimization problem. Observing the results of numerical integration, as time histories and phase diagrams, some interesting phenomena were verified, as for example bifurcation. Bifurcation is a typical nonlinear phenomena, and it is frequently discussed in many works (see for instance [73]). In the analyzed vibro-impact electromechanical system, it appears because depending on the values of the system parameters, the system response will have the occurrence or the non occurrence of impacts. But this topic is an ongoing research that will be object of a future work. The construction of the solution for the design optimization problem, has been prepared by carrying out a sensitivity analysis with respect all the possible design parameters. This pre-analysis has allowed for reducing the number of design parameters to two parameters. Consequently, a random search algorithm or a genetic algorithm was not necessary, and we have thus used a trail method. It should be noted that in the framework of a robust analysis formulated in the context of the probability theory, and taking into account the types of nonlinearities in the dynamical system, the Monte Carlo numerical simulation method has been used, and this introduces a significant increase of the numerical cost. The design optimization problem of the dynamical system without uncertainties yields an optimal design point that differs from the nominal values, and which can not be determined, *a priori*, without solving the design optimization problem. In addition, the robust analysis that has been presented demonstrates the interest that there is to take into account the uncertainties in the computational model. The optimal design point that has been identified in the robust design framework significantly differs from design point obtained with the computational model without uncertainties. For this electromechanical system, it has been seen that, the minimum value of the dispersion of the random output occurs in the region of the optimal design parameters, which means that the optimal design point is robust with respect to uncertainties.